Cis-acting lnc-Cxcl2 restrains neutrophil-mediated lung inflammation by inhibiting epithelial cell CXCL2 expression in virus infection

Shuo Liu[a,b], Jiaqi Liu[b], Xue Yang[b], Minghong Jiang[b], Qingqing Wang[a], Lianfeng Zhang[c], Yuanwu Ma[c], Zhongyang Shen[d], Zhigang Tian[e], and Xuetao Cao[a,b,f,1]

[a]Institute of Immunology, Zhejiang University School of Medicine, Hangzhou 310058, China; [b]Department of Immunology, Institute of Basic Medical Sciences, Peking Union Medical College, Chinese Academy of Medical Sciences, Beijing 100005, China; [c]Institute of Laboratory Animal Sciences, Chinese Academy of Medical Sciences, Beijing 100021, China; [d]Institute of Transplantation Medicine, Tianjin First Central Hospital, Nankai University, Tianjin 300070, China; [e]Institute of Immunology, School of Life Sciences and Medical Center, University of Science and Technology of China, Hefei 230027, China; and [f]College of Life Sciences, Nankai University, Tianjin 300071, China

Edited by Akiko Iwasaki, Yale University, New Haven, CT, and approved August 16, 2021 (received for review May 2, 2021)

Chemokine production by epithelial cells is important for neutrophil recruitment during viral infection, the appropriate regulation of which is critical for restraining inflammation and attenuating subsequent tissue damage. Epithelial cell expression of long noncoding RNAs (lncRNAs), RNA-binding proteins, and their functional interactions during viral infection and inflammation remain to be fully understood. Here, we identified an inducible lncRNA in the *Cxcl2* gene locus, lnc-Cxcl2, which could selectively inhibit *Cxcl2* expression in mouse lung epithelial cells but not in macrophages. lnc-Cxcl2–deficient mice exhibited increased *Cxcl2* expression, enhanced neutrophils recruitment, and more severe inflammation in the lung after influenza virus infection. Mechanistically, nucleus-localized lnc-Cxcl2 bound to *Cxcl2* promoter, recruited a ribonucleoprotein La, which inhibited the chromatin accessibility of chemokine promoters, and consequently inhibited *Cxcl2* transcription in *cis*. However, unlike mouse lnc-Cxcl2, human lnc-CXCL2-4-1 inhibited multiple immune cytokine expressions including chemokines in human lung epithelial cells. Together, our results demonstrate a self-protecting mechanism within epithelial cells to restrain chemokine and neutrophil-mediated inflammation, providing clues for better understanding chemokine regulation and epithelial cell function in lung viral infection.

chemokine CXCL2 | lung inflammation | neutrophil | epithelial cell

Chemokine production and chemokine-mediated neutrophil recruitment are critical for the elimination of invading pathogens and also determination of the infection outcome: homeostasis or inflammation (1, 2). High levels of chemokines and neutrophil recruitment have been found strongly correlated with the inflammatory tissue damage and fetal outcome of viral infection including influenza virus infection and the current pandemic coronavirus disease 2019 (COVID-19) (3–5). Besides, strategies that target the production of proinflammatory cytokines, chemokines, or downstream signaling have shown potential to suppress inflammation in COVID-19 (6, 7), reminding the urgent need for better understanding of the mechanism of chemokine expression and regulation in viral infectious diseases.

Chemokines that recruit neutrophils are mainly in the CXCL8 family, including CXCL1, CXCL2, and CXCL8 (human) (8). Epithelial cells, as the barrier between host and environment, play important roles in producing these chemokines (9, 10), especially in the respiratory tract where epithelial cells are the primary targets of many pathogens, including influenza virus and coronavirus (11–13). Moreover, a recently described human oral mucosa cell atlas has linked epithelial cells with inflammatory signatures to enhanced neutrophil recruitment during oral tissue inflammation (14). Thus, timely and appropriate regulation of chemokine expression in epithelial cells is critical for preventing inflammatory tissue damage while defending against the invading pathogens. However, the negative regulation of chemokines production in epithelial cells and its underlying mechanism remain to be elucidated in the interaction of host and pathogens, especially during lung viral infection.

Long noncoding RNAs (lncRNAs) can regulate gene expression at multiple levels in different physiological and pathological conditions (15). LncRNAs are classified into *cis*-acting and *trans*-acting according to the location of their transcription sites relative to their target positions. *Cis*-acting lncRNAs function as local effectors to regulate the expression of their neighboring genes, and many coexpressed neighboring messenger RNA (mRNA)–lncRNA pairs with positive correlation have been identified (16–18). However, whether *cis*-acting lncRNAs participate in the negative regulation of chemokine expression in epithelial cells and their potential functions in virus-induced inflammation remain to be investigated. Besides, interaction between RNA and RNA-binding proteins (RBPs) has been shown to play critical roles in the RNA-mediated regulation of transcription (19, 20). Thus, we wanted to identify *cis*-acting lncRNAs that transcribed near chemokine genes and their

Significance

Epithelial cell–mediated chemokine production and subsequent neutrophil recruitment are important for pathogen clearance, which, however, are also closely related to severe inflammatory tissue damage during lung infection, especially influenza virus infection and the current pandemic coronavirus infection. Certain regulation and underlying mechanisms of chemokine expression in epithelial cells remain largely unknown. Here, by identifying the mouse long noncoding RNA lnc-Cxcl2 and human lnc-CXCL2-4-1 in virus-infected lung epithelial cells, we demonstrated a self-protecting mechanism in host lung epithelial cells for restraining viral infection–induced lung inflammation through feedback-suppressing chemokine expression. These findings provide better understandings of chemokine regulation and epithelial cell function during lung viral infection and will benefit the treatment of related lung infectious diseases.

Author contributions: X.C. designed research; S.L., J.L., X.Y., M.J., Q.W., L.Z., and Y.M. performed research; Z.S. and Z.T. contributed new reagents/analytic tools; S.L. and X.C. analyzed data; S.L. and X.C. wrote the paper; and Z.S. and Z.T. provided helpful discussion.

The authors declare no competing interest.

This article is a PNAS Direct Submission.

[1]To whom correspondence may be addressed. Email: caoxt@immunol.org.

This article contains supporting information online at https://www.pnas.org/lookup/suppl/doi:10.1073/pnas.2108276118/-/DCSupplemental.

Published October 4, 2021.

possible interactive RBPs in lung epithelial cells and tried to demonstrate their functions in virus infection–induced inflammation.

By analyzing lncRNA expression profile in virus-infected mouse lung epithelial cells, we identified an inducible lncRNA in the *Cxcl2* gene locus, which we designated as lnc-Cxcl2, which could restrain neutrophil-mediated lung inflammation in a feedback manner during influenza virus infection. We demonstrated that the *cis*-acting lnc-Cxcl2 bound to the promoter of *Cxcl2* and recruited the ribonucleoprotein La to inhibit the transcription of *Cxcl2* in lung epithelial cells. However, we also found that unlike mouse lnc-Cxcl2, which acted in *cis*, human lnc-CXCL2-4-1 inhibited the expression of multiple cytokines including chemokines by binding La in human lung epithelial cells during influenza virus infection. Together, our findings uncover an epigenetic mechanism for inhibiting epithelial cell chemokine expression and attenuating lung inflammation during viral infection.

Results

lnc-Cxcl2 Expression Is Increased in the Nucleus of Mouse Lung Epithelial Cells in Response to Viral Infection. To investigate whether *cis*-acting lncRNAs participate in the regulation of *Cxcl2* expression in epithelial cells during viral infection, we infected mouse lung epithelial cells (MLE-12 cells) with recombinant vesicular stomatitis virus (VSV) expressing GFP (GFP-VSV), collected GFP-positive cells 12 h later, and analyzed lncRNA expression profile by RNA sequencing. We focused on lncRNAs expressed near chemokine genes, which may function as local effectors, and found that the expression level of the *Cxcl2* locus (Gene identity: ENSMUSG00000058427; chr5:90903870-90905938) in virus-infected lung epithelial cells was significantly higher than that in noninfected cells, indicating that there might be new transcripts within this region. Indeed, by using rapid amplification of complementary DNA (cDNA) ends (RACE) analysis, we found two previously uncharacterized transcripts in *Cxcl2* gene locus, the longer transcript had 1,660 nucleotides (nt) whereas the shorter one had 977 nt (*SI Appendix*, Fig. S1 *A* and *B* and Table S1). These two transcripts had a same 5′ end started from the intron 2 region of *Cxcl2*, shared the same sequence with pre-mRNA of *Cxcl2* containing the intron 3, and contained polyA signals in 3′ ends, which makes them different from the pre-mRNA of *Cxcl2* (*SI Appendix*, Fig. S1 *A* and *B*). Moreover, analyses using Coding Potential Calculator (21) and Open Reading Frame Finder showed that both transcripts lacked coding potential (*SI Appendix*, Fig. S1 *C* and *D*). We thereafter designated the long and the short transcripts as lncRNA of *Cxcl2* locus (lnc-Cxcl2).

To characterize lnc-Cxcl2, we first observed that the expression of lnc-Cxcl2 was increased in MLE-12 cells, primary mouse alveolar epithelial cells (AECs), and trachea epithelial cells (TECs) in response to both influenza A virus (IAV) and VSV infection (Fig. 1 *A*–*D*). By using Northern blot analysis, we found that both transcripts of lnc-Cxcl2 were induced in MLE-12 cells after VSV infection (Fig. 1*E*). We further calculated the absolute copy number of lnc-Cxcl2 and found that lnc-Cxcl2 has 15 ± 3 copies per uninfected MLE-12 cell and could reach up to 164 ± 8 copies after VSV infection (*SI Appendix*, Fig. S1*E*). In addition to epithelial cells, lnc-Cxcl2 expression was also increased in virus-infected mouse resident alveolar macrophages (AMs) and RAW264.7 cells (*SI Appendix*, Fig. S1 *F* and *G*).

To further investigate the cellular localization of lnc-Cxcl2, we separated different cell compartments and found that lnc-Cxcl2 was mainly located in the nucleus of MLE-12 cells (*SI Appendix*, Fig. S1*H*). Consistently, in situ hybridization analysis confirmed that lnc-Cxcl2 was located in the nucleus and its expression was increased after VSV infection (Fig. 1*F*). Then, we wondered how lnc-Cxcl2 was induced in response to viral infection. We found that addition of the NF-κB inhibitor reduced the expression of both *Cxcl2* and lnc-Cxcl2 in response to viral infection (Fig. 1 *G* and *H*), indicating that lnc-Cxcl2, like *Cxcl2*, was induced via the NF-κB signaling pathway. Together, these results demonstrate that lnc-Cxcl2 is a nuclear lncRNA whose expression is increased in mouse lung epithelial cells in response to viral infection.

lnc-Cxcl2 Selectively Inhibits *Cxcl2* Expression in Lung Epithelial Cells during Viral Infection. To investigate whether lnc-Cxcl2 regulated the expression of *Cxcl2* during viral infection, we generated lnc-Cxcl2–deficient (*lnc-Cxcl2*$^{-/-}$) MLE-12 cells using the CRISPR-Cas9 system (*SI Appendix*, Fig. S2*A*). *lnc-Cxcl2*$^{-/-}$ cells showed the same proliferation rate and similar proportion of cell death after VSV infection as wild-type (*lnc-Cxcl2*$^{+/+}$) MLE-12 cells (*SI Appendix*, Fig. S2 *B* and *C*).

However, by performing transcriptome analysis, we found 21 genes dysregulated in *lnc-Cxcl2*$^{-/-}$ cells after viral infection (Fig. 2*A* and *SI Appendix*, Table S2), and *Cxcl2* was among the up-regulated genes (Fig. 2*B* and *SI Appendix*, Table S2). Consistent with the transcriptome analysis data, we found that the *Cxcl2* expression in *lnc-Cxcl2*$^{-/-}$ cells and the secreted CXCL2 level in the *lnc-Cxcl2*$^{-/-}$ cell supernatant were increased compared to those in *lnc-Cxcl2*$^{+/+}$ cells in response to viral infection (Fig. 2 *C* and *D*). However, the expression of monocyte chemokine *Ccl2*, interferon *Ifnb1*, proinflammatory cytokine *Tnf*, and the other neutrophil chemokine *Cxcl3* were not obviously changed (*SI Appendix*, Fig. S2 *D* and *E*).

As tissue resident macrophage-derived chemokines also control the early recruitment of neutrophils in tissue inflammation (22), we detected whether lnc-Cxcl2 inhibited *Cxcl2* expression in macrophages. By generating *lnc-Cxcl2*$^{-/-}$ RAW264.7 cells, we found that although lnc-Cxcl2 expression was increased after VSV infection, lnc-Cxcl2 deficiency did not change *Cxcl2* expression in RAW264.7 cells (*SI Appendix*, Fig. S2*F*), indicating that lnc-Cxcl2 might selectively inhibit *Cxcl2* expression in mouse lung epithelial cells but not in macrophages. To test this hypothesis, we generated *lnc-Cxcl2*$^{-/-}$ mice using CRISPR-Cas9 system (*SI Appendix*, Fig. S3*A*) and isolated primary AECs, TECs, and AMs from these mice. We found that lnc-Cxcl2 deficiency increased *Cxcl2* expression in both IAV- and VSV-infected AECs and TECs but not in AMs (Fig. 2*E* and *SI Appendix*, Fig. S3*B*). Thus, these results demonstrate that lnc-Cxcl2 selectively inhibits *Cxcl2* expression in mouse lung epithelial cells during viral infection.

lnc-Cxcl2 Restrains Influenza Virus–Induced Lung Inflammation In Vivo. We next investigated the in vivo function of lnc-Cxcl2. *lnc-Cxcl2*$^{-/-}$ mice were viable, fertile, and almost indistinguishable from *lnc-Cxcl2*$^{+/+}$ littermates in appearance, body weight, and behavior. And the proportions of immune cells, including T cells, B cells, natural killer cells, neutrophils, macrophages, and dendritic cells in the spleen of *lnc-Cxcl2*$^{+/+}$ and *lnc-Cxcl2*$^{-/-}$ mice were also similar (*SI Appendix*, Fig. S3*C*), suggesting that lnc-Cxcl2 deficiency did not affect immune cell development in mice. Then, we intranasally infected these mice with IAV, which targeted lung epithelial cells for infection and induced lung inflammation and tissue damage. We found that *lnc-Cxcl2*$^{-/-}$ mice showed more body weight loss compared to *lnc-Cxcl2*$^{+/+}$ mice after IAV infection (Fig. 3*A*). And the expression of *Cxcl2* but not other proinflammatory cytokines, like *Ccl2*, *Ifnb1*, or *Tnf*, in the lung of *lnc-Cxcl2*$^{-/-}$ mice was increased compared to *lnc-Cxcl2*$^{+/+}$ mice after IAV infection, although viral load in the lungs was similar (Fig. 3*B*). Besides, the CXCL2 level and neutrophil numbers in the bronchoalveolar lavage fluid (BALF) of *lnc-Cxcl2*$^{-/-}$ mice were higher than that of *lnc-Cxcl2*$^{+/+}$ mice (Fig. 3 *C* and *D*). Consistent with that, *lnc-Cxcl2*$^{-/-}$ mice had more neutrophil infiltration, more severe inflammation, and tissue damage in the lung compared to *lnc-Cxcl2*$^{+/+}$ mice after IAV infection (Fig. 3 *E* and *F*). However, the expression of *Cxcr2* in bone marrow neutrophils from *lnc-Cxcl2*$^{+/+}$ and *lnc-Cxcl2*$^{-/-}$ mice was similar (*SI Appendix*, Fig. S3*D*), suggesting that more

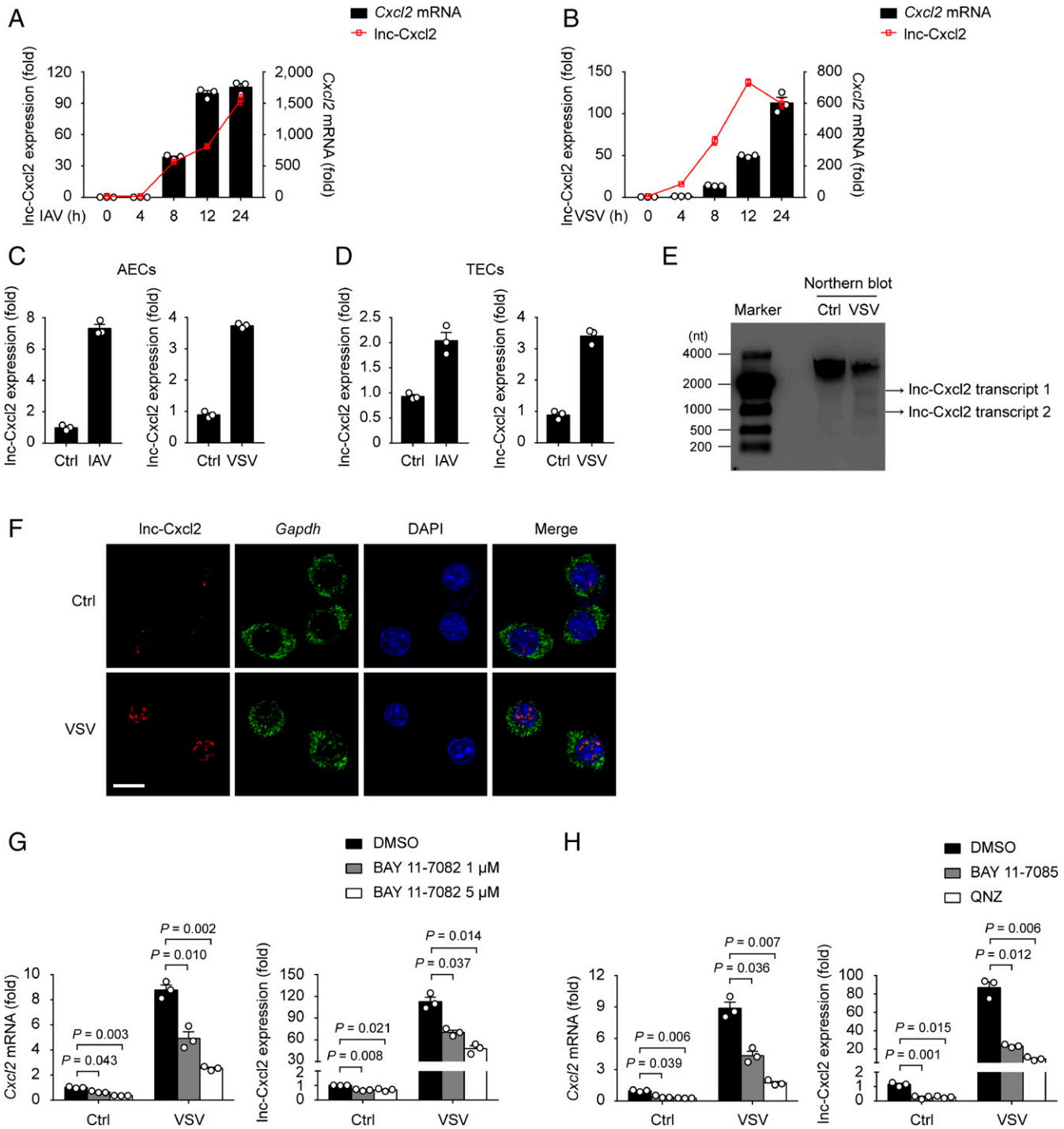

Fig. 1. lnc-Cxcl2 expression is increased in the nucleus of mouse lung epithelial cells in response to viral infection. (*A* and *B*) qPCR analysis of lnc-Cxcl2 and *Cxcl2* mRNA expressions in MLE-12 cells infected with IAV (multiplicity of infection [MOI] = 1) (*A*) or VSV (MOI = 1) (*B*) for indicated hours. (*C* and *D*) qPCR analysis of lnc-Cxcl2 expression in AECs (*C*) and TECs (*D*) infected with IAV (MOI = 1) or VSV (MOI = 1) for 12 h. (*E*) Northern blot analysis of lnc-Cxcl2 in MLE-12 cells infected with VSV (MOI = 1) for 12 h. (*F*) RNA in situ hybridization analysis of lnc-Cxcl2 and *Gapdh* in MLE-12 cells infected with VSV (MOI = 1) for 12 h. (Scale bar, 10 μm.) (*G*) qPCR analysis of *Cxcl2* mRNA and lnc-Cxcl2 expressions in MLE-12 cells treated with DMSO or BAY 11-7082 for 2 h followed by VSV infection (MOI = 1) for 12 h. (*H*) qPCR analysis of *Cxcl2* mRNA and lnc-Cxcl2 expressions in MLE-12 cells treated with DMSO, BAY 11-7085 (5 μM), or QNZ (EVP4593) (10 nM) for 2 h followed by VSV infection (MOI = 1) for 12 h. Data are representative of three independent experiments (*E* and *F*) or three independent experiments with $n = 3$ biological replicates (*A*–*D*, *G*, and *H*; shown as mean ± SEM in *A* and *B*, shown as mean + SEM in *C*, *D*, *G*, and *H*), two-tailed unpaired Student's *t* test. Ctrl, control.

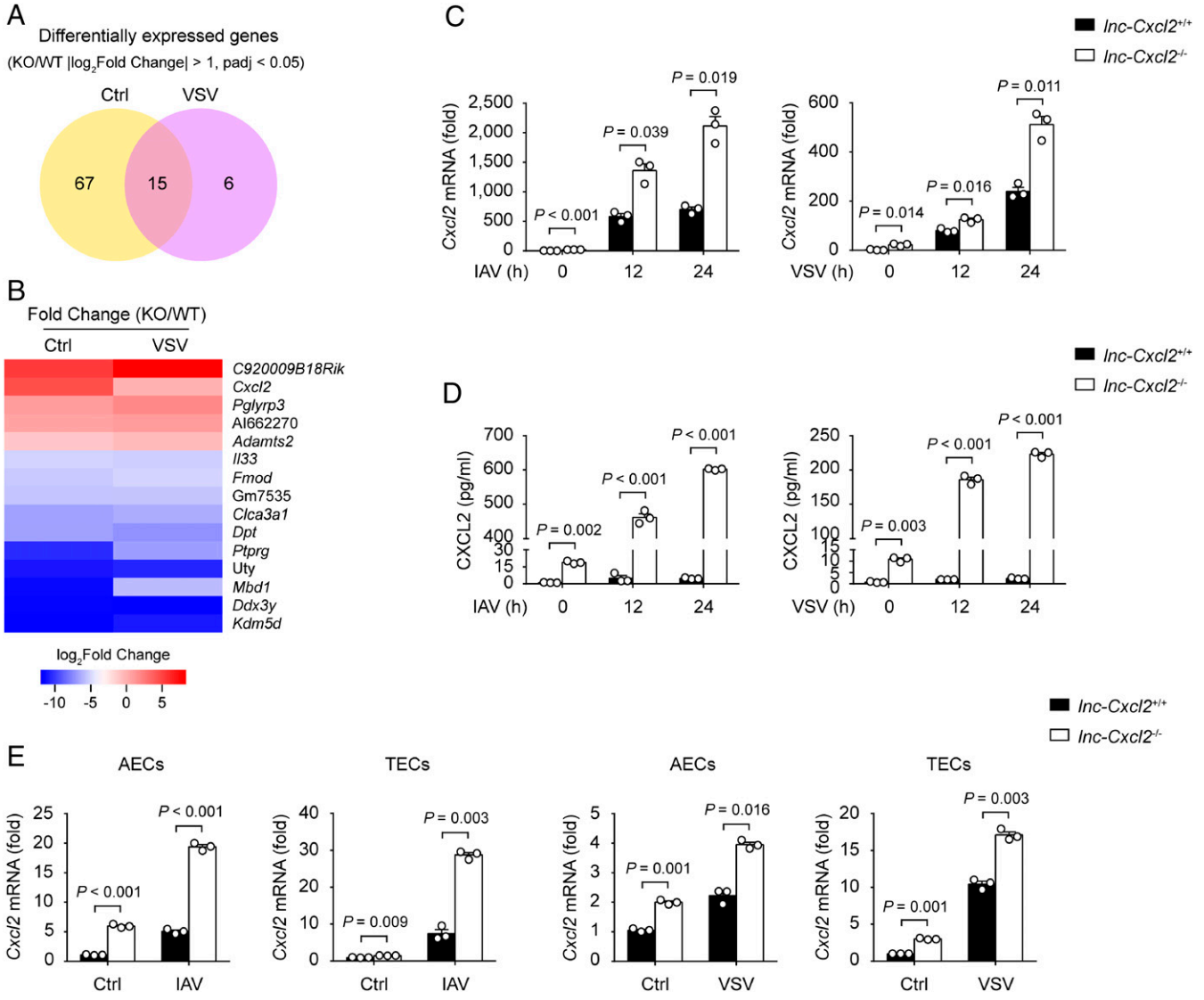

Fig. 2. lnc-Cxcl2 selectively inhibits *Cxcl2* expression in lung epithelial cells during viral infection. (*A*) Venn diagram of differentially expressed genes between *lnc-Cxcl2*$^{+/+}$ and *lnc-Cxcl2*$^{-/-}$ MLE-12 cells infected with VSV (multiplicity of infection [MOI] = 1) for 12 h. |log$_2$Fold Change| > 1 and adjusted *P* value (padj) < 0.05. WT, wild type; KO, knockout. (*B*) Heatmap of differentially expressed genes between *lnc-Cxcl2*$^{+/+}$ and *lnc-Cxcl2*$^{-/-}$ MLE-12 cells infected with VSV (MOI = 1) for 12 h. (*C*) qPCR analysis of *Cxcl2* mRNA expression in *lnc-Cxcl2*$^{+/+}$ and *lnc-Cxcl2*$^{-/-}$ MLE-12 cells infected with IAV (MOI = 1) or VSV (MOI = 1) for indicated hours. (*D*) Enzyme-linked immunosorbent assay of CXCL2 level in the supernatant of *lnc-Cxcl2*$^{+/+}$ and *lnc-Cxcl2*$^{-/-}$ MLE-12 cells infected with IAV (MOI = 1) or VSV (MOI = 1) for indicated hours. (*E*) qPCR analysis of *Cxcl2* mRNA expression in AECs and TECs from *lnc-Cxcl2*$^{+/+}$ and *lnc-Cxcl2*$^{-/-}$ mice infected with IAV (MOI = 1) or VSV (MOI = 1) for 12 h. Data are representative of three independent experiments with *n* = 3 biological replicates (*C* and *D*; shown as mean + SEM) or two independent experiments with *n* = 3 biological replicates (*E*; shown as mean + SEM), two-tailed unpaired Student's *t* test. Ctrl, control.

neutrophils recruited into the lung of *lnc-Cxcl2*$^{-/-}$ mice was due to the increased level of CXCL2.

To further demonstrate the function of lnc-Cxcl2, we infected mice with lower doses of IAV and monitored body weight and inflammation for 2 wk. We found that 2 wk after IAV infection, *lnc-Cxcl2*$^{-/-}$ mice had delayed weight recovery and increased *Cxcl2* expression in the lungs (*SI Appendix*, Fig. S3 *E* and *F*), which were accompanied by more neutrophil infiltration and unresolved inflammation compared to *lnc-Cxcl2*$^{+/+}$ mice (*SI Appendix*, Fig. S3*G*). Together, these results demonstrate that lnc-Cxcl2 restrains influenza virus–induced lung inflammation through inhibiting *Cxcl2* expression and neutrophil recruitment in vivo.

lnc-Cxcl2 Binds to and Maintains the Repressed Chromatin State of *Cxcl2* Promoter in *Cis*. We then investigated how lnc-Cxcl2 inhibited *Cxcl2* expression during viral infection. We examined signalings that participate in the expression of *Cxcl2* (23, 24) and found that lnc-Cxcl2 deficiency did not alter the nuclear localization of transcription factors like P65, P50, STAT1, STAT3, or c-JUN (*SI Appendix*, Fig. S4*A*). We wondered whether lnc-Cxcl2 regulated the transcription of *Cxcl2* in *cis*. We found that lnc-Cxcl2 deficiency increased the *Cxcl2* pre-mRNA level in response to viral infection (Fig. 4*A*), and the chromatin accessibility (indicated by DNase I sensitivity) of the *Cxcl2* promoter (indicated by two κB sites, *SI Appendix*, Fig. S4*B*) was increased in *lnc-Cxcl2*$^{-/-}$ cells in response to VSV infection (Fig. 4*B*). Consistently, the H3K4me3 and CREB binding protein (CBP) levels in *Cxcl2* promoter, which are two markers of active transcription, were increased in *lnc-Cxcl2*$^{-/-}$ cells in response to VSV infection (Fig. 4 *C* and *D*). The total and the phosphorylated RNA polymerase II levels in the *Cxcl2* promoter were also increased in *lnc-Cxcl2*$^{-/-}$ cells (Fig. 4 *E* and *F*), suggesting that

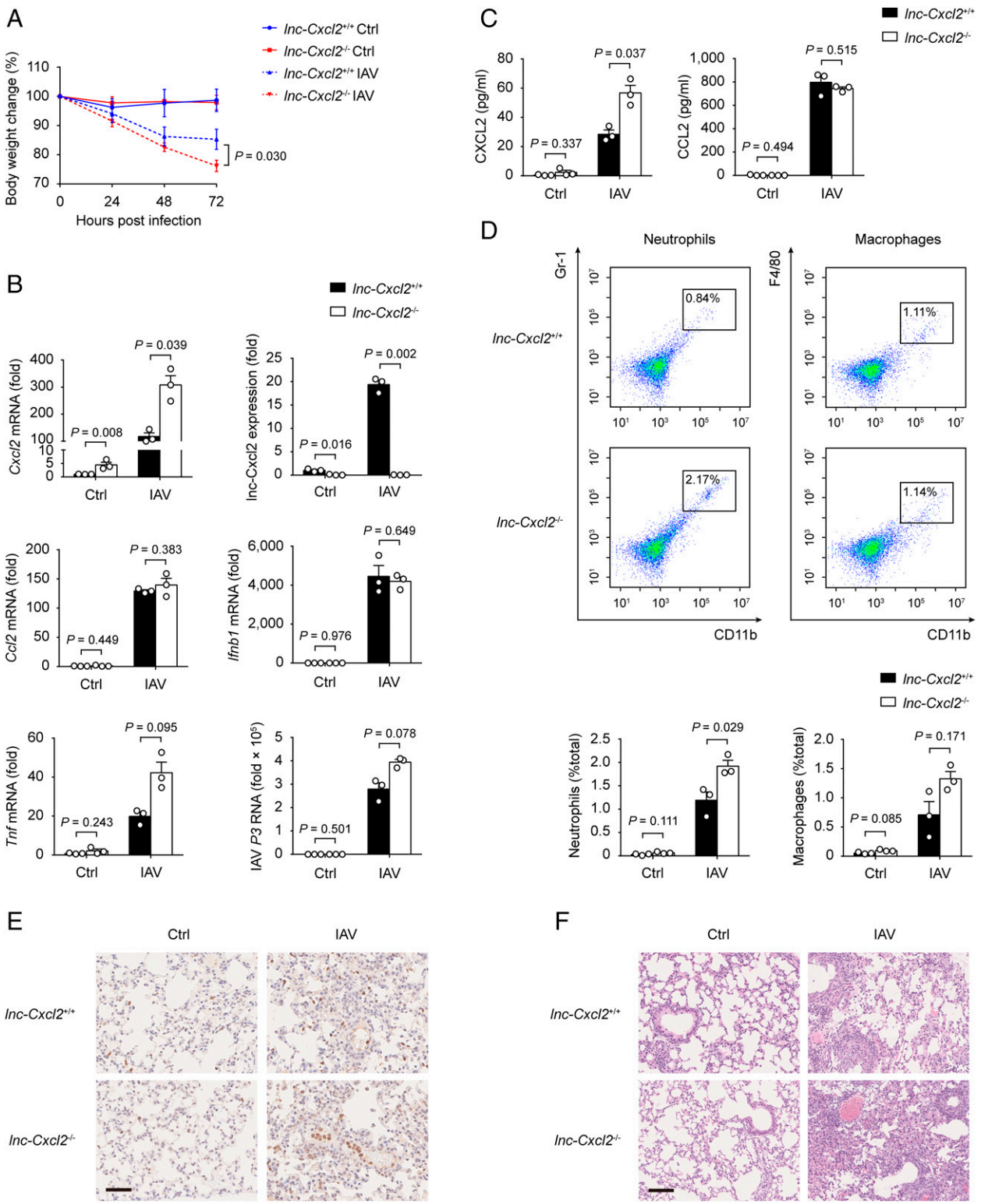

Fig. 3. Inc-Cxcl2 restrains influenza virus–induced lung inflammation in vivo. (*A*) Body weight change analysis of *Inc-Cxcl2*$^{+/+}$ and *Inc-Cxcl2*$^{-/-}$ mice intranasally infected with IAV (3×10^5 PFU) for 72 h. (*B*) qPCR analysis of *Cxcl2*, Inc-Cxcl2, *Ccl2*, *Ifnb1*, and *Tnf* mRNA expressions and IAV load indicated by virus polymerase P3 expression in lungs from mice described in *A*. (*C*) Enzyme-linked immunosorbent assay of CXCL2 and CCL2 levels in the BALF from mice described in *A*. (*D*) Flow cytometric analysis of CD11b$^+$Gr-1$^+$ neutrophil and CD11b$^+$F4/80$^+$ macrophage propagations in BALF from mice described in *A*. (*E*) Immunohistochemistry staining of Gr-1$^+$ neutrophils of lung sections from mice described in *A*. (Scale bar, 50 μm.) (*F*) Hematoxylin and eosin staining of lung sections from the mice described in *A*. (Scale bar, 100 μm.) Data are representative of three independent experiments with three mice per group (*A–F*; shown as mean ± SEM in *A*, shown as mean + SEM in *B–D*), two-way ANOVA analysis (*A*), two-tailed unpaired Student's *t* test (*B–D*). Ctrl, control.

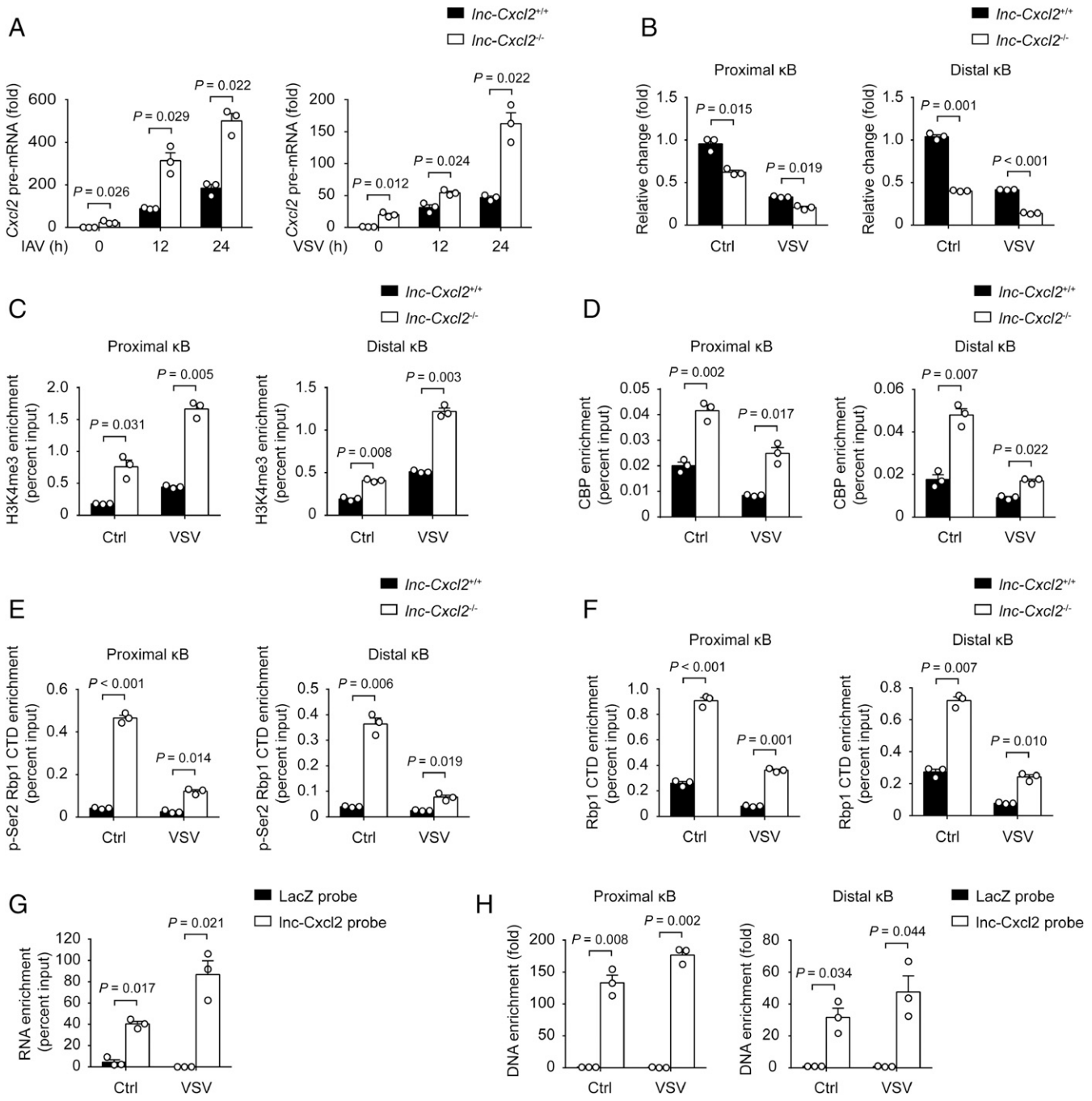

Fig. 4. lnc-Cxcl2 binds to and maintains the repressed chromatin state of *Cxcl2* promoter *in cis*. (*A*) qPCR analysis of *Cxcl2* pre-mRNA expression in *lnc-Cxcl2*$^{+/+}$ and *lnc-Cxcl2*$^{-/-}$ MLE-12 cells infected with IAV (multiplicity of infection [MOI] = 1) or VSV (MOI = 1) for indicated hours. (*B*) qPCR analysis of the DNase I sensitivity of the *Cxcl2* promoter in *lnc-Cxcl2*$^{+/+}$ and *lnc-Cxcl2*$^{-/-}$ MLE-12 cells infected with VSV (MOI = 1) for 12 h. (*C–F*) qPCR analysis of H3K4me3 (*C*), CBP (*D*), pSer2-RNA polymerase II carboxy-terminal domain (CTD) (*E*), and total RNA polymerase II CTD (*F*) enrichment levels in the *Cxcl2* promoter in *lnc-Cxcl2*$^{+/+}$ and *lnc-Cxcl2*$^{-/-}$ MLE-12 cells infected with VSV (MOI = 1) for 12 h. (*G*) qPCR analysis of lnc-Cxcl2 retrieved by antisense RNA probes in MLE-12 cells infected with VSV (MOI = 1) for 12 h. (*H*) qPCR analysis of enrichment level of *Cxcl2* promoter that purified by lnc-Cxcl2 probes in MLE-12 cells infected with VSV (MOI = 1) for 12 h. Data are representative of three independent experiments with $n = 3$ biological replicates (*A–F*; shown as mean + SEM) or from three independent experiments (*G* and *H*; shown as mean + SEM), two-tailed unpaired Student's *t* test. Ctrl, control.

lnc-Cxcl2 inhibited the chromatin accessibility of *Cxcl2* promoter and the transcription of *Cxcl2*. We further used small interfering RNA to silence the expression of lnc-Cxcl2 to further confirm the function of lnc-Cxcl2. As lnc-Cxcl2 shared the same sequence with pre-mRNA of *Cxcl2*, silencing the expression of lnc-Cxcl2 simultaneously down-regulated the expression of *Cxcl2* (*SI Appendix*, Fig. S4*C*). Nevertheless, silencing the expression of lnc-Cxcl2 increased the chromatin accessibility of the *Cxcl2* promoter compared to silencing the negative control (*SI Appendix*, Fig. S4*D*), indicating that lnc-Cxcl2 itself could inhibit the chromatin accessibility of the *Cxcl2* promoter.

To clarify how lnc-Cxcl2 regulated the chromatin accessibility of the *Cxcl2* promoter, we examined whether lnc-Cxcl2 could directly bind to the *Cxcl2* promoter. We isolated lnc-Cxcl2–binding

chromatin by RNA purification using antisense probes that specifically target lnc-Cxcl2. We found that the probes successfully captured lnc-Cxcl2 especially after VSV infection (Fig. 4*G*), and the two regions containing κB sites of the *Cxcl2* promoter were highly enriched in lnc-Cxcl2–binding DNA, whereas those of the *Ccl2* promoter were not (Fig. 4*H* and *SI Appendix*, Fig. S4*E*), indicating that lnc-Cxcl2 selectively bound to the promoter of *Cxcl2*. Together, these results demonstrate that lnc-Cxcl2 binds to *Cxcl2* promoter and maintains a repressed chromatin state of *Cxcl2* promoter in *cis* during viral infection.

lnc-Cxcl2 Inhibits *Cxcl2* Expression through Ribonucleoprotein La. We next investigated whether lnc-Cxcl2 inhibited the chromatin accessibility through its interactive proteins. Using RNA pull-down assay followed by mass spectrometry (MS) analysis, we identified 13 lnc-Cxcl2–interacting nuclear proteins (*SI Appendix*, Table S3). We examined whether these proteins were involved in the regulation of *Cxcl2* expression and found that only silencing the expression of *Ssb*, which encoded the ribonucleoprotein La, increased the expression of *Cxcl2* (*SI Appendix*, Fig. S5*A*). To test the hypothesis that lnc-Cxcl2 inhibited *Cxcl2* transcription through interacting with La, we first confirmed the interaction between lnc-Cxcl2 and La. We found that in vitro transcribed-lnc-Cxcl2 bound La but not transcription factor P65 or STAT3 (*SI Appendix*, Fig. S5*B*). Furthermore, by using antisense RNA probes to purify the endogenous lnc-Cxcl2 and its associated proteins, we found that lnc-Cxcl2 was associated with La in MLE-12 cells but not in RAW264.7 cells (Fig. 5*A* and *SI Appendix*, Fig. S5*C*). Conversely,

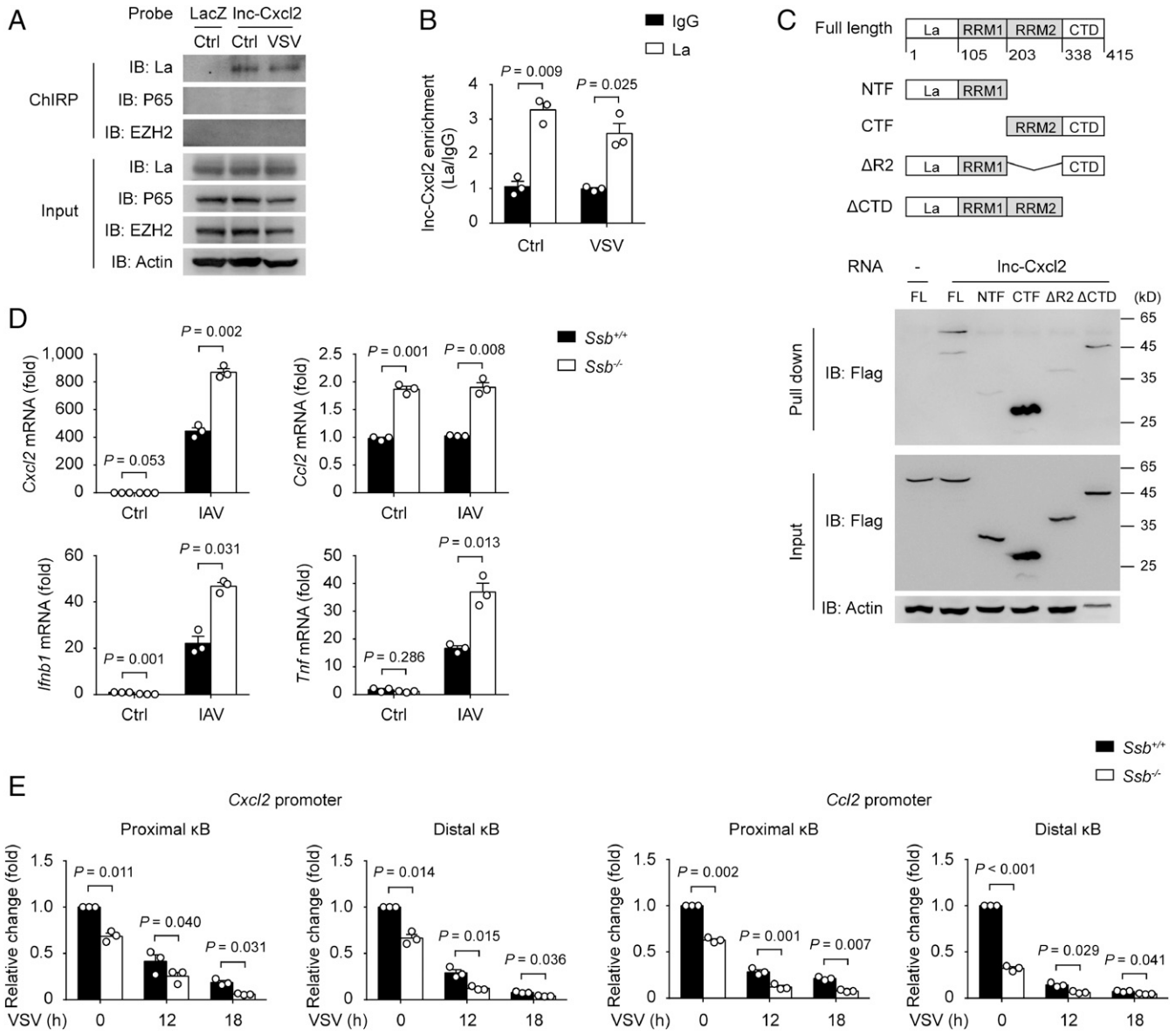

Fig. 5. lnc-Cxcl2 inhibits *Cxcl2* expression through ribonucleoprotein La. (*A*) Immunoblot analysis of proteins purified by lnc-Cxcl2 probes in MLE-12 cells infected with VSV (multiplicity of infection [MOI] = 1) for 12 h. (*B*) qPCR analysis of lnc-Cxcl2 level purified by La antibody in MLE-12 cells infected with VSV (MOI = 1) for 12 h. (*C*) Schematic illustration of La truncations (*Top*), and the immunoblot analysis of lnc-Cxcl2 and La truncations interaction in HEK293T cells transfected with Flag-tagged La truncations (*Bottom*). FL, full length. (*D*) qPCR analysis of *Cxcl2*, *Ccl2*, *Ifnb1*, and *Tnf* mRNA expressions in $Ssb^{+/+}$ and $Ssb^{-/-}$ MLE-12 cells infected with IAV (MOI = 1) for 12 h. (*E*) qPCR analysis of the DNase I sensitivity of *Cxcl2* and *Ccl2* promoters in $Ssb^{+/+}$ and $Ssb^{-/-}$ MLE-12 cells infected with VSV (MOI = 1) for indicated hours. Data are representative of three independent experiments (*A* and *C*) or three independent experiments with $n = 3$ biological replicates (*B*, *D*, and *E*; shown as mean + SEM), two-tailed unpaired Student's *t* test. Ctrl, control; IB, immunoblot.

immunoprecipitation analysis using antibody against La showed that endogenous La was associated with the endogenous lnc-Cxcl2 in MLE-12 cells (Fig. 5*B*).

La contains an N-terminal La motif, two RNA recognition motifs (RRM), and a C-terminal nuclear localization signal (25). The binding preference of the La motif and RRM1 domain in the N terminus correlates with the cellular localization of La: They recognize the UUU-3′OH of pre–transfer RNAs in the nucleus, whereas they recognize the poly(A) tail of mRNAs in the cytoplasm (26, 27). However, the function of the C-terminal part of La, especially the second RRM, has not been identified clearly. To detect which domain of La interacted with lnc-Cxcl2, we expressed different La truncations and found that only La fragments containing the second RRM bound to lnc-Cxcl2, suggesting that La interacted with lnc-Cxcl2 through RRM2 (Fig. 5*C*).

To investigate the function of La in regulating *Cxcl2* expression, we generated La-deficient ($Ssb^{-/-}$) MLE-12 cells (*SI Appendix*, Fig. S5*D*). To our surprise, La deficiency not only increased the expression of *Cxcl2* but also other chemokines and proinflammatory cytokines, like *Ccl2*, *Ifnb1*, and *Tnf* in response to viral infection (Fig. 5*D* and *SI Appendix*, Fig. S5*E*). Then, we examined how La inhibited the expressions of these cytokines and found that La deficiency increased the chromatin accessibility of *Cxcl2* and *Ccl2* promoters (Fig. 5*E*). To clarify how La inhibited the chromatin accessibility, we tried to find La-interacting nuclear proteins using MS analysis. A total of 34 proteins were identified to interact with La in MLE-12 cells (*SI Appendix*, Table S4). Gene ontology analysis showed that the molecular functions of most of these proteins were linked to RNA binding and ribosome structure (*SI Appendix*, Fig. S5*F*), indicating that La might inhibit these cytokine transcriptions through forming an RBP complex and ribosomal protein complex in mouse epithelial cells. Together, although La inhibits the expressions of many cytokines, lnc-Cxcl2 can bind to the *Cxcl2* promoter and inhibit *Cxcl2* expression in *cis* through ribonucleoprotein La during viral infection.

lnc-CXCL2-4-1 Inhibits Immune Cytokine Expressions in Human Lung Epithelial Cells. Although lncRNAs have been characterized as low conserved between different species, we asked whether a similar mechanism exists in human cells. By searching lncRNA databases, four transcripts related to *CXCL2* were found in the downstream of human *CXCL2*, including lnc-CXCL2-1-1, lnc-CXCL2-2-1, lnc-CXCL2-3-1, and lnc-CXCL2-4-1 (28, 29). Among these, lnc-CXCL2-3-1 was predicted to have coding probability (29), thus only the other three transcripts were considered as noncoding RNAs; however, the detailed function of these three lncRNAs has not been clarified yet. Therefore, we first examined the expression of these lncRNAs in A549 human lung epithelial cells and found that the expression of lnc-CXCL2-4-1 was dramatically increased after IAV infection whereas the expressions of lnc-CXCL2-1-1 and lnc-CXCL2-2-1 were only slightly increased (Fig. 6*A*). We then tested whether lnc-CXCL2-4-1 participated in the regulation of chemokine expression. By performing transcriptome analysis, 364 genes were found to be up-regulated and 32 down-regulated in lnc-CXCL2-4-1–silenced A549 cells after IAV infection (Fig. 6B). Gene ontology analysis of these differentially expressed genes showed their molecular functions were enriched in cytokine activity, including chemokines, interferons, and other proinflammatory cytokines (Fig. 6 *C* and *D*). We further confirmed that silencing the expression of lnc-CXCL2-4-1 indeed increased the expression of *CXCL2* and *CXCL8* in A549 cells after IAV infection (Fig. 6*E*). We then wondered whether lnc-CXCL2-4-1 inhibited these cytokine expressions by binding La. We found that lnc-CXCL2-4-1 interacted with La, and silencing the expression of La increased both *CXCL2* and *CXCL8* expressions in A549 cells after IAV infection (Fig. 6 *F* and *G*), indicating that lnc-CXCL2-4-1 inhibited cytokine expressions through binding La in human lung epithelial cells.

To further demonstrate the different regulatory function of mouse lnc-Cxcl2 and human lnc-CXCL2-4-1, we compared the secondary structure of these two lncRNAs. We found that although mouse lnc-Cxcl2 and human lnc-CXCL2-4-1 both have multiple stem loops in their secondary structure, human lnc-CXCL2-4-1 formed more stem-loop clusters, which might facilitate its regulation of multiple gene expression (*SI Appendix*, Fig. S6).

Taken together, these results demonstrate a host self-protecting mechanism in different species for restraining virus-induced lung inflammation through increasing the expression of an lncRNA, which can feedback inhibit chemokine production in lung epithelial cells.

Discussion

Epithelial cells act as the first line in defending against pathogens and maintaining homeostasis of regional tissue such as the lungs. The levels of epithelial cell–derived chemokines and subsequent neutrophil recruitment are closely related to the severity of many inflammatory diseases including infection, stress, asthma, and even cancer metastasis (30–32); thus, our findings of the inducible lncRNA, which can attenuate inflammatory damage through feedback inhibition of lung epithelial cell chemokine expression and neutrophil recruitment, will benefit not only the control of respiratory viral infections but also other related lung inflammatory diseases.

We demonstrate that lnc-Cxcl2 selectively inhibits *Cxcl2* expression in epithelial cells but not in macrophages, indicating that a cell type–specific molecular mechanism may exist for lnc-Cxcl2, possibly relying on different intracellular and extracellular signals and metabolism-shaped chromatin architecture during viral infection. Thus, further investigations still need to be done to elucidate the selective role of lnc-Cxcl2 in different cells, especially by generating cell type–specific deficient mice. Besides, we also demonstrate that mouse lnc-Cxcl2 and human lnc-CXCL2-4-1 have different regulating profiles. Mouse lnc-Cxcl2 is located in the *Cxcl2* gene locus and transcription factors, chromatin remodelers, and other nuclear proteins nearby may combine to facilitate it to regulate its neighboring gene expression in *cis*. However, human lnc-CXCL2-4-1 is located in the downstream of *CXCL2* gene locus, which does not make it that easy to target to one specific chromatin site but rather to regulate multiple gene expression. These differences between cells and species indicate the complexity of lncRNA evolution and function, which needs to be considered in future studies.

We demonstrate that lnc-Cxcl2 inhibits *Cxcl2* expression through binding La. La has been reported to associate with RNA polymerase III–transcribed genes and act as an initiation and termination factor for RNA polymerase III (33). However, whether and how La regulates RNA polymerase II–mediated transcription remains unclear. A previous study has found that conditional deletion of La in the mouse brain increases the expression of multiple immune genes, including chemokines (34). Consistent with this, we demonstrate that deletion of La in lung epithelial cells increases the expression of chemokines, interferons, and also some other proinflammatory cytokines during viral infection, confirming the regulating function of La in the RNA polymerase II–mediated transcription. Besides, our MS analysis suggests that La inhibits gene expression through forming two protein groups: the RBP group and ribosome structure protein group. As an RBP, it is possible for La to interact with other RBPs to assemble into RNP complexes (35). Cotranscriptional assembly of RNP complex is important for the maintenance of genome integrity by preventing the formation of R-loop during transcription (35, 36), which might simultaneously suppress the chromatin accessibility and shut down the transcription. On the other hand, noncanonical function of ribosome constituents in gene expression has also been found. Ribosomal protein S3 is an essential subunit of the NF-κB and can facilitate

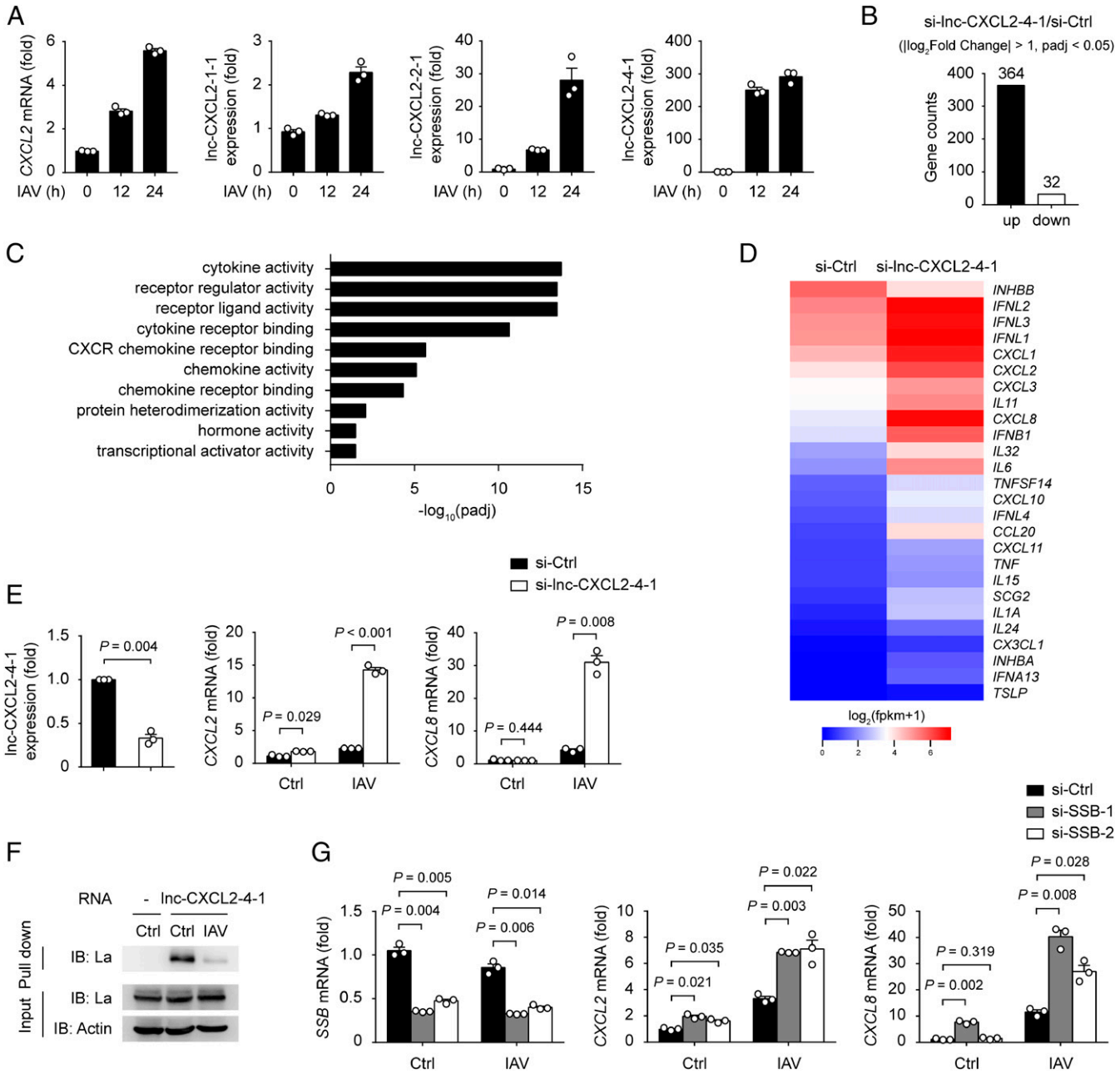

Fig. 6. lnc-CXCL2-4-1 inhibits cytokine expressions in human lung epithelial cells. (*A*) qPCR analysis of *CXCL2* mRNA, lnc-CXCL2-1-1, lnc-CXCL2-2-1, and lnc-CXCL2-4-1 expressions in A549 cells infected with IAV (multiplicity of infection [MOI] = 1) for indicated hours. (*B*) Differentially expressed gene numbers between negative control (Ctrl) small interfering RNA (siRNA) and lnc-CXCL2-4-1 siRNA-transfected A549 cells infected with IAV (MOI = 1) for 12 h. $|\log_2\text{Fold Change}| > 1$ and adjusted *P* value (padj) < 0.05. (*C*) Gene ontology analysis of differentially expressed genes between negative ctrl siRNA and lnc-CXCL2-4-1 siRNA-transfected A549 cells infected with IAV (MOI = 1) for 12 h. Top 10 enriched molecular function gene ontology terms are shown (padj < 0.05). (*D*) Heatmap of differentially expressed cytokine genes between negative ctrl siRNA and lnc-CXCL2-4-1 siRNA-transfected A549 cells infected with IAV (MOI = 1) for 12 h. $|\log_2\text{Fold Change}| > 1$ and adjusted *P* value (padj) < 0.05. (*E*) qPCR analysis of lnc-CXCL2-4-1, *CXCL2*, and *CXCL8* mRNA expressions in A549 cells transfected with negative ctrl siRNA or lnc-CXCL2-4-1 siRNA (100 nM) followed by IAV infection (MOI = 1) for 12 h. (*F*) Immunoblot analysis of lnc-CXCL2-4-1 and La interaction in A549 cells infected with IAV (MOI = 1) for 12 h. (*G*) qPCR analysis of *SSB*, *CXCL2*, and *CXCL8* mRNA expressions in A549 cells transfected with negative ctrl siRNA or *SSB* siRNA (20 nM) followed by IAV infection (MOI = 1) for 12 h. Data are representative of three independent experiments (*F*) or three independent experiments with $n = 3$ biological replicates (*A*, *E*, and *G*; shown as mean + SEM), two-tailed unpaired Student's *t* test. Ctrl, control; IB: immunoblot.

the selective control of gene expression by NF-κB (37). Suppressing the biogenesis of ribosome by interfering with ribosomal RNA accumulation can impair interferon expression without suppressing translation (38). Therefore, further study could focus on how La inhibits cytokine expression through binding these two protein complexes, and demonstrating this mechanism will greatly help understanding the function of La in inflammation and also autoimmune diseases more than just as an autoantigen.

Except for La, we also identify several other RBPs that interact with lnc-Cxcl2. Among them, the proteins which participated in RNA transcription and splicing are mostly enriched, like Ddx21, Ddx5, Ilf2, Tial1, Ybx1, and Eif4a3, suggesting that lnc-Cxcl2 may be processed through binding these proteins. Besides, some

heterogeneous nuclear ribonucleoproteins (hnRNPs) that have been reported to participate in lncRNA-mediated gene regulation are also found, like hnRNPab, which can regulate *Cxcl2* expression in bone marrow–derived macrophages (39). However, we did not detect the same effect of hnRNPab in MLE-12 cells, indicating that the function of hnRNPs may also be cell type specific. In addition, other proteins involved in gene regulation in different cells are also detected, like Eef1a1 which regulates gene expression in myelinating cells (40), while Pcbp1 promotes proinflammatory cytokine expression in T cells (41). Interaction with these proteins provides other functional possibilities for lnc-Cxcl2, and it will be worthy to investigate the role of lnc-Cxcl2 under different physiological and pathological conditions in the future.

Materials and Methods

Mice and Cell Lines. C57BL/6 mice were from Beijing Vital River Laboratory (Beijing, China). lnc-Cxcl2–deficient mice were generated using the CRISPR-Cas9 system on a C57BL/6 background. Briefly, two guide RNAs respectively targeting the upstream of exon 3 (5′-TGGCCAGAGTTGCCCAGA-3) and downstream of exon 4 (5′-CTAACTGACCTGGAAAGG-3′) of *Cxcl2* and a donor plasmid containing the sequence of exon 3 and exon 4 of *Cxcl2* were used to delete the intron 3 of *Cxcl2* and consequently delete lnc-Cxcl2. The genotypes of offspring mice were determined by PCR using the following primers: F: 5′-TTGCCTTGACCCTGAAGC-3′; R: 5′-GTACGATCCAGGCTTCCC-3′.

All mice were maintained in specific pathogen-free conditions. All mouse experiments were performed under the supervision of Institutional Animal Care and Use Committee, Institute of Basic Medical Sciences, Chinese Academy of Medical Sciences, Beijing, China (ACUC-A01-2017-004).

MLE-12 cells, RAW264.7 cells, human embryonic kidney cells (HEK293T cells), and A549 cells were from ATCC. lnc-Cxcl2–deficient MLE-12 cells and RAW264.7 cells were generated using guide RNAs targeting the intron 3 of *Cxcl2*: 5′-TCATTTGGAAAGGTTCAAGC-3′ and 5′-AGGCTAGAGATGGTTTCGTT-3′ for MLE-12 cells and 5′-ATCAAGGTTAACTTCAGTTC-3′ and 5′-AGGCTAGAGATGGTTTCGTT-3′ for RAW264.7 cells. La-deficient MLE-12 cells were generated using two guide RNAs targeting the exon 5 of *Ssb*: 5′-CATCAAGGGTGGCGTCAGTT-3′ and 5′-AAAGAATGGCTAGACGATAA-3′.

5′ and 3′ RACE. A 5′ and 3′ RACE of lnc-Cxcl2 was performed using SMARTer RACE 5′/3′ Kit (Clontech Laboratories) following the manufacturer's instructions. The cDNA template was from MLE-12 cells infected with VSV for 12 h. Primers used were as follows: 5′-R1:5′-GCTGGCGTTACAATTGTACCAGCTTGAACC-3′; 5′-R2: 5′-AGCGAGAGCCTACACCTGAATTTCAAGCCTC-3′; 3′-F1: 5′-CCTTCCTTAATGGATGGTCGCTGTGTGTCCC-3′; and 3′-F2: 5′-CCCCTGCCCTTTCCATGTCTGTGGGCTG-3′.

Northern Blot. Total RNA was extracted from MLE-12 cells infected with VSV for 12 h; then, 20 μg RNA was used for electrophoresis in 1.5% denaturing agarose gel. After that, RNA was transferred to nylon membrane and crosslinked by ultraviolet light. The cross-linked membrane was prehybridized using PerfectHyb Plus hybridization buffer (Sigma-Aldrich) and further hybridized overnight by adding biotin-labeled RNA probes to the hybridization buffer. After wash, the membrane was exposed using Chemiluminescent Nucleic Acid Detection Module (Thermo Scientific) following the manufacturer's instructions. Biotin-labeled RNA probes were synthesized by in vitro transcription using T7 RNA Polymerase and Biotin RNA Labeling Mix (Roche). The DNA template used to transcribe RNA probes was amplified according to lnc-Cxcl2 cDNA using the following primers: 5′-GGAAAGGTTCAAGCTGGTACAA-3′ and 5′-TAATACGACTCACTATAGGGACCTTGGTTTACTCTCCAAA-3′.

RNA In Situ Hybridization Assay. MLE-12 cells were seeded into an eight-chambered dish and infected with VSV for 12 h. After infection, cells were fixed with 4% paraformaldehyde followed by permeabilization with 0.2% Triton X-100 in phosphate-buffered saline. Then, specific probe pools were used to hybridize lnc-Cxcl2, and Stellaris fluorescent in situ hybridization probes (Biosearch Technologies) were used to hybridize *Gapdh* mRNA in Stellaris hybridization buffer (Biosearch Technologies). Finally, nuclei were stained with DAPI. The fluorescence of RNA and nuclei were detected by Leica TCS SP8 gSTED 3X. The probes targeting lnc-Cxcl2 were as follows: 5′-ATTTTCAGAAATCGGGTGCC-3′, 5′-TGAAAGGAGCTAGTCGTACC-3′, 5′-TGACTTCGCGTACGTTGTAA-3′, 5′-CTGGGCGCTTTGAAACTAGA-3′, 5′-GGACTTTCCAGCAATAAACA-3′, 5′-AGTGGGTATCTTAAAGGCGG-3′, 5′-GGAAGGACTTTTACGTGTGT-3′, and 5′-AGATAACAGGCTTTACACCA-3′.

Influenza Virus Infection Model. Six- to eight-week-old *lnc-Cxcl2*$^{+/+}$ and *lnc-Cxcl2*$^{-/-}$ littermates with the same gender were used. For IAV infection, mice were first anesthetized using tribromoethanol intraperitoneally (0.25 mg/g body weight) and then intranasally inoculated with IAV (3×10^5 plaque-forming units [PFU] in 30 μL solution or 50 PFU in 20 μL solution). Mice in the control group were also anesthetized and intranasally administrated with solution instead. The body weight of all mice was measured every 24 h. After infection for indicated times, BALF was collected for cell infiltration and cytokine analysis; lung tissue was collected for RNA extraction and histopathological examination.

Chromatin Isolation by RNA Purification. Chromatin isolation by RNA purification (ChIRP) assay was performed using Magna ChIRP RNA Interactome Kit (Millipore) following the manufacturer's instructions with some modifications. In brief, cells were harvested and crosslinked with 1% formaldehyde. Then, the 100-mg cell pellet was resuspended in lysis buffer and sonicated to shear DNA. For lnc-Cxcl2–linked chromatin or protein isolation, 100 pmol biotin-labeled probe mix and streptavidin magnetic beads were added to hybridize and capture lnc-Cxcl2 separately. Obtained bead samples were divided into two parts, one for DNA or protein isolation and detection, the other for RNA isolation and quantification. The probes used to hybridize lnc-Cxcl2 were designed by ChIRP Probe Designer from LGC Biosearch Technologies, and the sequences were as follows: 5′-TTTCTTTAGGGTGAGCATGG-3′; 5′-TTCAGGGTCAAGGCAAACTT-3′; 5′-ATTTTCAGAAATCGGGTGCC-3′; 5′-TCGTACCCTTCTATCAATTC-3′; 5′-CGCTAGTTGGTTCTATCTAC-3′; 5′-AGTTAGACTTTACAGCCCAC-3′; 5′-CTGAATTTCAAGCCTCTCAC-3′; 5′-GACTTCGCGTACGTTGTAAA-3′; 5′-CTAGAATAGTAGAGCTGGCG-3′; 5′-AACGAAACCATCTCTAGCCT-3′; 5′-TTGCTGTTAGTGGGTATCTT-3′; and 5′-TCTTTGGTTCTTCCGTTGAG-3′.

Statistical Analysis. Comparisons of data from two groups were performed using two-tailed unpaired Student's *t* test. Comparisons of mouse body weight and cell proliferation data with different time points between two groups were performed using two-way ANOVA analysis. *P* values less than 0.05 were considered as statistically significant.

Data Availability. The RNA sequencing data from this study have been deposited in the National Center for Biotechnology Information Gene Expression Omnibus under accession code GSE156949 and GSE179951 (42, 43). All other study data are included in the article and/or *SI Appendix*.

ACKNOWLEDGMENTS. This work was supported by grants from the National Natural Science Foundation of China (81788101 and 81930041) and Chinese Academy of Medical Sciences Innovation Fund for Medical Sciences (2016-12M-1-003).

1. J. W. Griffith, C. L. Sokol, A. D. Luster, Chemokines and chemokine receptors: Positioning cells for host defense and immunity. *Annu. Rev. Immunol.* **32**, 659–702 (2014).
2. E. Kolaczkowska, P. Kubes, Neutrophil recruitment and function in health and inflammation. *Nat. Rev. Immunol.* **13**, 159–175 (2013).
3. R. Alon *et al.*, Leukocyte trafficking to the lungs and beyond: Lessons from influenza for COVID-19. *Nat. Rev. Immunol.* **21**, 49–64 (2021).
4. M. Laforge *et al.*, Tissue damage from neutrophil-induced oxidative stress in COVID-19. *Nat. Rev. Immunol.* **20**, 515–516 (2020).
5. B. M. Tang *et al.*, Neutrophils-related host factors associated with severe disease and fatality in patients with influenza infection. *Nat. Commun.* **10**, 3422 (2019).
6. M. Buszko *et al.*, The dynamic changes in cytokine responses in COVID-19: A snapshot of the current state of knowledge. *Nat. Immunol.* **21**, 1146–1151 (2020).
7. X. Cao, COVID-19: Immunopathology and its implications for therapy. *Nat. Rev. Immunol.* **20**, 269–270 (2020).
8. C. L. Sokol, A. D. Luster, The chemokine system in innate immunity. *Cold Spring Harb. Perspect. Biol.* **7**, a016303 (2015).
9. A. Iwasaki, E. F. Foxman, R. D. Molony, Early local immune defences in the respiratory tract. *Nat. Rev. Immunol.* **17**, 7–20 (2017).
10. R. Lehmann *et al.*, Differential regulation of the transcriptomic and secretomic landscape of sensor and effector functions of human airway epithelial cells. *Mucosal Immunol.* **11**, 627–642 (2018).
11. K. H. Benam, L. Denney, L. P. Ho, How the respiratory epithelium senses and reacts to influenza virus. *Am. J. Respir. Cell Mol. Biol.* **60**, 259–268 (2019).
12. R. B. Polidoro, R. S. Hagan, R. de Santis Santiago, N. W. Schmidt, Overview: Systemic inflammatory response derived from lung injury caused by SARS-CoV-2 infection explains severe outcomes in COVID-19. *Front. Immunol.* **11**, 1626 (2020).
13. Z. Qian *et al.*, Innate immune response of human alveolar type II cells infected with severe acute respiratory syndrome-coronavirus. *Am. J. Respir. Cell Mol. Biol.* **48**, 742–748 (2013).

14. D. W. Williams *et al*.; NIDCD/NIDCR Genomics and Computational Biology Core, Human oral mucosa cell atlas reveals a stromal-neutrophil axis regulating tissue immunity. *Cell* **184**, 4090–4104.e15 (2021).
15. L. Statello, C. J. Guo, L. L. Chen, M. Huarte, Gene regulation by long non-coding RNAs and its biological functions. *Nat. Rev. Mol. Cell Biol.* **22**, 96–118 (2021).
16. N. Gil, I. Ulitsky, Regulation of gene expression by cis-acting long non-coding RNAs. *Nat. Rev. Genet.* **21**, 102–117 (2020).
17. N. Khyzha *et al*., Regulation of *CCL2* expression in human vascular endothelial cells by a neighboring divergently transcribed long noncoding RNA. *Proc. Natl. Acad. Sci. U.S.A.* **116**, 16410–16419 (2019).
18. I. Sarropoulos, R. Marin, M. Cardoso-Moreira, H. Kaessmann, Developmental dynamics of lncRNAs across mammalian organs and species. *Nature* **571**, 510–514 (2019).
19. Y. Long *et al*., RNA is essential for PRC2 chromatin occupancy and function in human pluripotent stem cells. *Nat. Genet.* **52**, 931–938 (2020).
20. R. Xiao *et al*., Pervasive chromatin-RNA binding protein interactions enable RNA-based regulation of transcription. *Cell* **178**, 107–121.e18 (2019).
21. L. Kong *et al*., CPC: Assess the protein-coding potential of transcripts using sequence features and support vector machine. *Nucleic Acids Res.* **35**, W345-9 (2007).
22. K. De Filippo *et al*., Mast cell and macrophage chemokines CXCL1/CXCL2 control the early stage of neutrophil recruitment during tissue inflammation. *Blood* **121**, 4930–4937 (2013).
23. S. J. Burke *et al*., NF-κB and STAT1 control CXCL1 and CXCL2 gene transcription. *Am. J. Physiol. Endocrinol. Metab.* **306**, E131–E149 (2014).
24. M. Jaramillo, M. Olivier, Hydrogen peroxide induces murine macrophage chemokine gene transcription via extracellular signal-regulated kinase- and cyclic adenosine 5′-monophosphate (cAMP)-dependent pathways: Involvement of NF-kappa B, activator protein 1, and cAMP response element binding protein. *J. Immunol.* **169**, 7026–7038 (2002).
25. C. Alfano *et al*., Structural analysis of cooperative RNA binding by the La motif and central RRM domain of human La protein. *Nat. Struct. Mol. Biol.* **11**, 323–329 (2004).
26. S. A. Marrella *et al*., An interdomain bridge influences RNA binding of the human La protein. *J. Biol. Chem.* **294**, 1529–1540 (2019).
27. J. Vinayak *et al*., Human La binds mRNAs through contacts to the poly(A) tail. *Nucleic Acids Res.* **46**, 4228–4240 (2018).
28. L. Zhao *et al*., NONCODEV6: An updated database dedicated to long non-coding RNA annotation in both animals and plants. *Nucleic Acids Res.* **49**, D165–D171 (2021).
29. P. J. Volders *et al*., LNCipedia 5: Towards a reference set of human long non-coding RNAs. *Nucleic Acids Res.* **47**, D135–D139 (2019).
30. A. Frey *et al*., More than just a barrier: The immune functions of the airway epithelium in asthma pathogenesis. *Front. Immunol.* **11**, 761 (2020).
31. N. Hernández-Santos *et al*., Lung epithelial cells coordinate innate lymphocytes and immunity against pulmonary fungal infection. *Cell Host Microbe* **23**, 511–522.e5 (2018).
32. Y. Liu *et al*., Tumor exosomal RNAs promote lung pre-metastatic niche formation by activating alveolar epithelial TLR3 to recruit neutrophils. *Cancer Cell* **30**, 243–256 (2016).
33. J. A. Fairley *et al*., Human La is found at RNA polymerase III-transcribed genes in vivo. *Proc. Natl. Acad. Sci. U.S.A.* **102**, 18350–18355 (2005).
34. N. H. Blewett, J. R. Iben, S. Gaidamakov, R. J. Maraia, La deletion from mouse brain alters pre-tRNA metabolism and accumulation of Pre-5.8S rRNA, with neuron death and reactive astrocytosis. *Mol. Cell. Biol.* **37**, e00588–e16 (2017).
35. A. Montecucco, G. Biamonti, Pre-mRNA processing factors meet the DNA damage response. *Front. Genet.* **4**, 102 (2013).
36. K. Nishida, Y. Kuwano, T. Nishikawa, K. Masuda, K. Rokutan, RNA binding proteins and genome integrity. *Int. J. Mol. Sci.* **18**, 1341 (2017).
37. F. Wan *et al*., Ribosomal protein S3: A KH domain subunit in NF-kappaB complexes that mediates selective gene regulation. *Cell* **131**, 927–939 (2007).
38. C. Bianco, I. Mohr, Ribosome biogenesis restricts innate immune responses to virus infection and DNA. *eLife* **8**, e49551 (2019).
39. S. Carpenter *et al*., A long noncoding RNA mediates both activation and repression of immune response genes. *Science* **341**, 789–792 (2013).
40. M. Duman *et al*., EEF1A1 deacetylation enables transcriptional activation of remyelination. *Nat. Commun.* **11**, 3420 (2020).
41. Z. Wang *et al*., Iron drives T helper cell pathogenicity by promoting RNA-binding protein PCBP1-mediated proinflammatory cytokine production. *Immunity* **49**, 80–92.e7 (2018).
42. S. Liu, J. Liu, X. Yang, M. Jiang, X. Cao, lnc-Cxcl2 suppressed Cxcl2 expression in mouse lung epithelial cells. *Gene Expression Omnibus*. https://www.ncbi.nlm.nih.gov/geo/query/acc.cgi?acc=GSE156949. Deposited 27 August 2020.
43. S. Liu, J. Liu, X. Yang, X. Cao, Transcriptome analysis of genes that regulated by lnc-CXCL2-4-1. *Gene Expression Omnibus*. https://www.ncbi.nlm.nih.gov/geo/query/acc.cgi?acc=GSE179951. Deposited 12 July 2021.